Identification of Novel Nasopharyngeal Carcinoma Biomarkers by Laser Capture Microdissection and Proteomic Analysis

Ai-Lan Cheng,[1,3] Wei-Guo Huang,[1,3] Zhu-Chu Chen,[1,2] Fang Peng,[1] Peng-Fei Zhang,[1] Mao-Yu Li,[1] Feng Li,[1,2] Jian-Ling Li,[1] Cui Li,[1] Hong Yi,[1] Bin Yi,[1] and Zhi-Qiang Xiao[1]

Abstract

Purpose: To identify novel nasopharyngeal carcinoma (NPC) biomarkers by laser capture microdissection and a proteomic approach.

Experimental Design: Proteins from pooled microdissected NPC and normal nasopharyngeal epithelial tissues (NNET) were separated by two-dimensional gel electrophoresis, and differential proteins were identified by mass spectrometry. Expression of three differential proteins (stathmin, 14-3-3σ, and annexin I) in the above two tissues as well as four NPC cell lines was determined by Western blotting. Immunohistochemistry was also done to detect the expression of three differential proteins in 98 cases of primary NPC, 30 cases of NNET, and 20 cases of cervical lymph node metastases, and the correlation of their expression levels with clinicopathologic features and clinical outcomes were evaluated.

Results: Thirty-six differential proteins between the NPC and NNET were identified. The expression levels of stathmin, 14-3-3σ, and annexin I in the two types of tissues were confirmed and related to differentiation degree and/or metastatic potential of the NPC cell lines. Significant stathmin up-regulation and down-regulation of 14-3-3σ and annexin I were observed in NPC versus NNET, and significant down-regulation of 14-3-3σ and annexin I was also observed in lymph node metastasis versus primary NPC. In addition, stathmin up-regulation and down-regulation of 14-3-3σ and annexin I were significantly correlated with poor histologic differentiation, advanced clinical stage, and recurrence, whereas down-regulation of 14-3-3σ and annexin I was also significantly correlated with lymph node and distant metastasis. Furthermore, survival curves showed that patients with stathmin up-regulation and down-regulation of 14-3-3σ and annexin I had a poor prognosis. Multivariate analysis revealed that the expression status of stathmin, 14-3-3σ, and annexin I was an independent prognostic indicator.

Conclusion: The data suggest that stathmin, 14-3-3σ, and annexin I are potential biomarkers for the differentiation and prognosis of NPC, and their dysregulation might play an important role in the pathogenesis of NPC.

Nasopharyngeal carcinoma (NPC) is one of the most common malignant tumors in southern China and Southeast Asia, with an incidence rate ranging from 20 to 50/100,000 (1). Cantonese are the most frequently affected population, and the incidence rate of NPC in Cantonese is nearly 100-fold higher than that in Caucasians (2). This remarkable geographic and racial distribution of NPC indicates that the development of this cancer may be related to genetic and environmental factors.

A strong association between EBV and NPC has been widely accepted, which was initially suggested on the basis of serologic studies and has been subsequently substantiated by the detection of viral genomes and gene products in the tumor cells (2, 3). Multiple genetic and epigenetic alternations have been identified in NPC. For example, some inactivated tumor suppressor genes and activated oncogenes may be associated with NPC carcinogenesis (4, 5), aberrant hypermethylation of genes such as RASSF1A, RARβ2, and $p16^{INK4A}$ was identified in NPC (6), and frequent loss of heterozygosity on chromosomes 3p21-26, 3p13-14.3, and 9p21-22 was also detected in NPC (7–9). NPC susceptibility loci on chromosomes 4p15.1-q12 and 3p21.31-21.2 were recently identified by a genome-wide scan and a linkage analysis (10, 11). Although numerous efforts have been made to reveal the molecular mechanism of NPC carcinogenesis, it remains poorly understood. In this regard, the identification of NPC-associated proteins using a proteomic approach may be an alternative way for deciphering the molecular characteristics of the malignancy.

Authors' Affiliations: [1]Key Laboratory of Cancer Proteomics of Chinese Ministry of Health and Medical Research Center, Xiangya Hospital, and [2]Cancer Research Institute, Xiangya School of Medicine, Central South University, Changsha, China, and [3]Cancer Research Institute, University of South China, Hengyang, China
Received 5/17/07; revised 8/3/07; accepted 9/17/07.

Grant support: National Key Basic Research Program of China (2001CB510207), Outstanding Scholars of the New Era from the Ministry of Education of China (2002-48), and Key research program from the Science and Technology Committee of Hunan Province, China (04XK1001, 06SK2004).

The costs of publication of this article were defrayed in part by the payment of page charges. This article must therefore be hereby marked *advertisement* in accordance with 18 U.S.C. Section 1734 solely to indicate this fact.

Note: A-L. Cheng and W-G. Huang contributed equally to this work.

Requests for reprints: Zhi-Qiang Xiao, Key Laboratory of Cancer Proteomics of Chinese Ministry of Health, Xiangya Hospital, Central South University, Changsha 410008, Hunan Province, China. Phone: 86-731-4327239; Fax: 86-731-4327321; E-mail: zqxiao2001@hotmail.com.

doi:10.1158/1078-0432.CCR-07-1215

Although NPC is classified as a subtype of head and neck squamous cell carcinoma, its epidemiology, clinical characteristics, etiology, and histopathology are unique (2). For example, compared with other head and neck squamous cell carcinomas, NPC tends to present at a more advanced stage of disease because of its deep location and vague symptoms, exhibits higher metastatic potential, and its histologic grading related to radiosensitivity is more confusing (12). Furthermore, the survival rate for patients with NPC has remained unchanged in the past few years despite advances in diagnosis and treatment. Therefore, early diagnosis, exact histologic grading, and accurate prognostication of NPC are critical for guiding the treatment and improving the prognosis of NPC. The finding of NPC biomarkers may be a convenient way to achieve these objectives. With the advances in molecular biology in the past decades, a lot of NPC-related molecules, such as serum antibodies against various EBV proteins (13), serum amyloid A (14), Bmi-1 (15), and Met protein (16), etc., have been reported as potential biomarkers for the diagnosis, prognosis, or treatment of NPC. However, they are of limited clinical value because of low sensitivity or specificity. At present, the mainstay for the diagnosis and histologic grading of NPC is endoscopic examination and histologic observation of biopsies, and tumor-node-metastasis staging is still the main method of predicting the prognosis of NPC. Therefore, it is urgent to discover more effective biomarkers and therapeutic targets for NPC.

High-throughput technologies such as microarrays and proteomics offer the potential ability to find alterations previously unidentified in NPC. Analyses for gene expression profiles of NPC have been reported using a cDNA array, and found that genes with aberrant expressions possibly contributed to the pathogenesis of NPC (17). Proteomics has introduced a new approach to cancer research which aims at identifying differential expression proteins associated with the development and progression of cancer, providing new opportunities to uncover biomarkers and therapeutic targets for NPC as well as reveal the molecular mechanism underlying this disease. Using tissue samples from patients may be the most direct and persuasive way to find biomarkers and therapeutic targets for cancers by a proteomic approach. A major obstacle, however, to the analysis of tumor specimens is tissue heterogeneity, which is particularly relevant to NPC as it often includes numerous infiltrating lymphocytes and stroma. Moreover, normal nasopharyngeal epithelial cells, from which the cancer is believed to arise, represent as little as 10% of nasopharyngeal mucosal tissue. Several approaches have been employed to obtain homogeneous cell populations from a heterogeneous tissue for proteomic analysis, such as short-term cell culture, and laser capture microdissection (LCM). Since 1996, LCM has emerged as a good choice for purifying cells from tissue (18). There have been reports concerning proteomic research of laser capture–microdissected tumor cells such as breast (19), hepatocellular (20), and pancreatic cancers (21).

In the present study, LCM was used to isolate pure cell populations from NPC and normal nasopharyngeal epithelial tissue (NNET) samples, and two-dimensional gel electrophoresis (2-DE) and mass spectrometry (MS) were done to identify differential expression proteins between the two types of tissues. Because the expression levels of three differential proteins (stathmin, 14-3-3σ, and annexin I) in the two types of tissues were confirmed and related to the differentiation degree and/or metastatic potential of the NPC cell lines, the clinicopathologic significance of the three proteins were further evaluated using immunohistochemistry of paraffin-embedded archival tissue specimens and statistical analysis. Our findings provide substantial evidence that stathmin, 14-3-3σ, and annexin I are potential biomarkers for the differentiation and prognosis of NPC, and their dysregulation might play an important role in the development and progression of NPC. To our knowledge, this is the first differential proteomic analysis of NPC using microdissected cancer and normal cells. Our data will facilitate an understanding of NPC carcinogenesis and mining biomarkers for the diagnosis and treatment of this disease.

Materials and Methods

Materials. Immobiline pH gradient (IPG) DryStrips (pH 3-10 L, 24 cm), IPG buffer (pH 3-10), DryStrip cover fluids, thiourea, urea, CHAPS, DTT, Pharmalyte (pH 3-10), bromophenol blue, Bis, TEMED, Coomassie brilliant blue G-250, molecular weight marker, Tris-base, SDS, glycine, second antibodies conjugated with horseradish peroxidase, and the enhanced chemiluminescence system were purchased from Amersham Biosciences. Sequencing-grade modified trypsin was obtained from Promega. Polyvinylidene difluoride membrane and ZipTip C^{18} columns were obtained from Millipore. Mouse monoclonal antibody against stathmin was from Cell Signaling Technology, Inc. Goat polyclonal antibody against 14-3-3σ was from Santa Cruz Biotechnology. Rabbit polyclonal antibody against annexin I was from Abcam, Inc. Mercaptoethanol, iodoacetamide, α-cyano-4-hydroxycinnamic acid, and HCl were from Sigma-Aldrich. All buffers were prepared with Milli-Q water.

Tissues. Forty-two cases of fresh undifferentiated NPC (WHO type III) tissues and 42 cases of fresh NNET from healthy individuals were obtained from the First and Second Xiangya Hospitals of Central South University and the Cancer Hospital of Hunan Province, China at the time of diagnosis before any therapy, and used for 2-DE and Western blotting. The patients and healthy individuals signed an informed consent form for the study which was reviewed by the Institutional Review Board. All tissue samples were verified by histopathology before microdissection. An additional group of formalin-fixed and paraffin-embedded archival tissue specimens including 98 cases of primary NPC, 30 cases of NNET, and 20 cases of cervical lymph node metastatic NPC (LMNPC) between 1996 and 2000 were obtained from the Cancer Hospital of Hunan Province, and used for immunohistochemistry. According to the 1978 WHO classification (22), 98 cases of primary tumors were histopathologically diagnosed as keratinizing squamous cell carcinoma (WHO type I, 5 cases), differentiated nonkeratinizing squamous cell carcinoma (WHO type II, 13 cases), and undifferentiated carcinoma (WHO type III, 80 cases), and all LMNPC were undifferentiated carcinoma. The clinical stage of all the patients was classified or reclassified according to the 1992 NPC staging system of China (16). All the patients underwent radiotherapy treatment and were given follow-up. The follow-up period at the time of analysis was 6 to 72 months (average, 48 ± 14.5). The clinicopathologic features of the patients used in the present study are shown in Table 3.

Tissue processing and LCM. Eight-micrometer-thick frozen sections of fresh NPC and NNET were prepared using a Leica CM 1900 cryostat (Leica) at -25°C. The sections were placed on a membrane-coated glass slides (2.0 μm, 50 pieces, PEF Membrane; Leica), fixed in 75% alcohol for 30 s, and stained with 0.5% violet-free methyl green (Sigma). All solutions for staining were supplemented with protease inhibitor cocktail tablets (Roche Molecular Biochemicals). Following staining, the sections were air-dried and microdissected by a Leica AS LMD

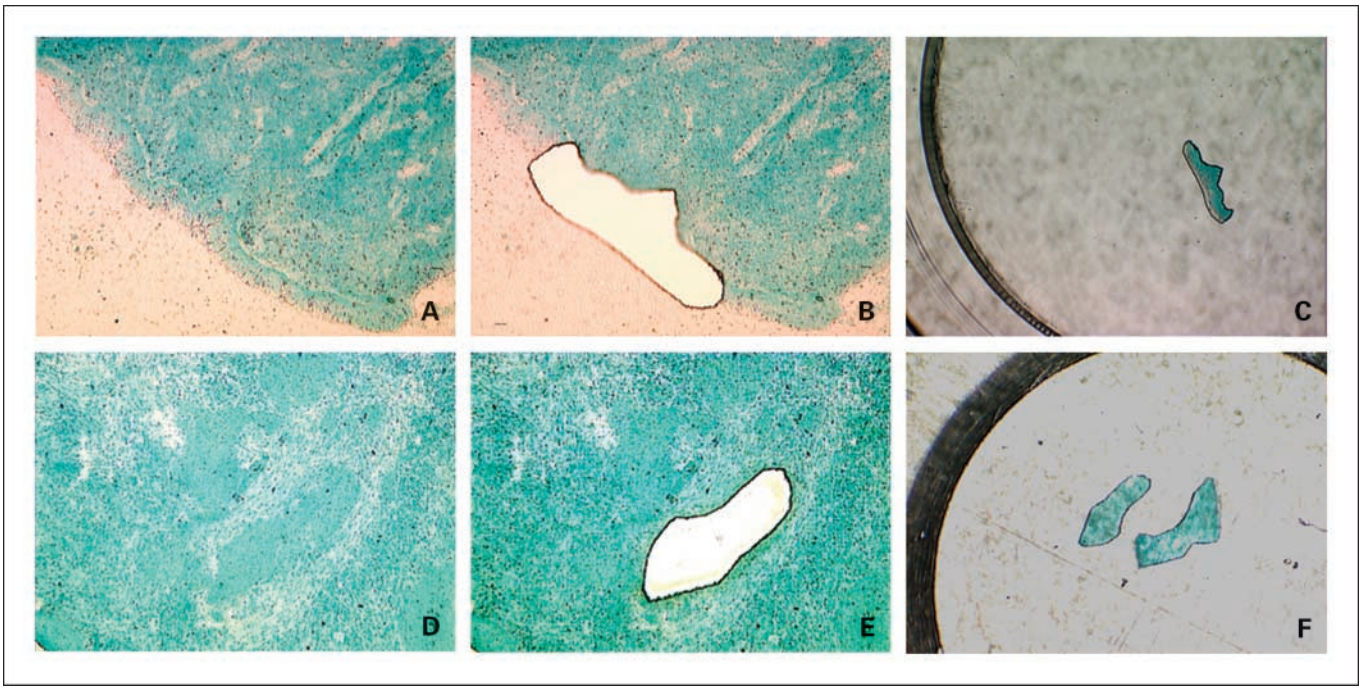

Fig. 1. LCM of tissues. NNET before (*A*) and after (*B*) LCM, and captured normal cells (*C*). NPC tissue before (*D*) and after (*E*) LCM, and captured cancer cells (*F*).

system (Leica). Approximately 200,000 to 250,000 microdissected cells were required for each 2-DE, and 20,000 to 25,000 microdissected cells were required for each Western blotting. As biopsy tissue specimens from one patient were too small to microdissect enough cells for one-time 2-DE, pooled microdissected cells from 10 NPC or 10 normal specimens were used for each 2-DE. Each cell population was determined to be 95% homogeneous by microscopic visualization of the captured cells (Fig. 1). The microdissected cells were dissolved in lysis buffer (7 mol/L urea, 2 mol/L thiourea, 100 mmol/L DTT, 4% CHAPS, 0.5 mmol/L EDTA, 40 mmol/L Tris, 2% NP40, 1% Triton X-100, 5 mmol/L phenylmethylsulfonyl fluoride, and 2% Pharmalyte) at 4°C for 1 h, and then centrifuged at 12,000 rpm for 30 min at 4°C. The supernatant was transferred to a fresh tube, and stored at -80°C until 2-DE. The concentration of the total proteins was measured by 2-D quantification kit (Amersham Biosciences).

Two-dimensional electrophoresis. 2-DE was done to separate proteins from three sets of pooled microdissected NPC and NNET as previously described by us (23). Briefly, 650 μg of protein samples were diluted to 450 μL with a rehydration solution [7 mol/L urea, 2 mol/L thiourea, 0.2% DTT, 0.5% (v/v) pH 3-10 IPG buffer, and trace bromophenol blue], and applied to IPG strips (pH 3-10L, 24 cm) by 14 h rehydration at 30 V. The proteins were focused successively for 1 h at 500 V, 1 h at 1,000 V, and 8.5 h at 8,000 V to give a total of 68 kVh on an IPGphor (Amersham Biosciences). Focused IPG strips were equilibrated for 15 min in a solution [6 mol/L urea, 2% SDS, 30% glycerol, 50 mmol/L Tris-HCl (pH 8.8), and 1% DTT], and then for an additional 15 min in the same solution except that DTT was replaced by 2.5% iodoacetamide. After equilibration, SDS-PAGE was done on Ettan DALT II system (Amersham Biosciences). After SDS-PAGE, the Blue Silver staining method, a modified Neuhoff's colloidal Coomassie blue G-250 stain, was used to visualize the protein spots in the 2-DE gels (24).

Image analysis. The stained 2-DE gels were scanned with MagicScan software on an Imagescanner (Amersham Biosciences), and analyzed by using a PDQuest system (Bio-Rad Laboratories) according to the protocols provided by the manufacturer. Three separate gels were prepared for each microdissected tissue. The gel spot pattern of each gel was summarized in a standard after spot matching. Thus, we obtained one standard gel for each tissue. Spot intensities were quantified by calculation of spot volume after normalization of the image using the total spot volume normalization method multiplied by the total area of all the spots. The change index was defined as the ratio between the spot percentage relative volumes in the microdissected tumor and normal tissues. Proteins were classified as being differentially expressed between the two types of tissues when spot intensity showed a difference of ≥2-fold variation in tumor tissue in comparison to normal tissue. Significant differences in protein expression levels were determined by Student's t test with a set value of $P < 0.05$.

Protein identification by MS. All the differential protein spots were excised from stained gels using punch, and in-gel trypsin digestion was done as previously described by us (23). The tryptic peptide was mixed with a α-cyano-4-hydroxycinnamic acid matrix solution. One microliter of the mixture was analyzed with a Voyager System DE-STR 4307 MALDI-TOF mass spectrometer (ABI) to obtain a peptide mass fingerprint. In peptide mass fingerprint map database searching, Mascot Distiller was used to obtain the monoisotopic peak list from the raw mass spectrometry files. Peptide matching and protein searches against the Swiss-Prot database were done using the Mascot search engine[4] with a mass tolerance of ±50 ppm. The protein spots identified by MALDI-TOF-MS were also subjected to analysis of ESI-Q-TOF-MS (Micromass; Waters). Briefly, the samples were loaded onto a precolumn (320 μm × 50 mm, 5 μm C18 silica beads; Waters) at 30 μL/min flow rates for concentrations and fast desalting through a Waters CapLC autosampler, and then eluted to the reversed-phase column (75 μm × 150 mm, 5 μm, 100 Å; LC Packing) at a flow rate of 200 nL/min after flow splitting for separation. MS/MS spectra were done in data-dependent mode in which up to four precursor ions above an intensity threshold of seven counts/s were selected for MS/MS analysis from each survey "scan." In tandem mass spectrometry data database query, the peptide sequence tag (PKL) format file that was generated from MS/MS was

[4] http://www.matrixscience.com/

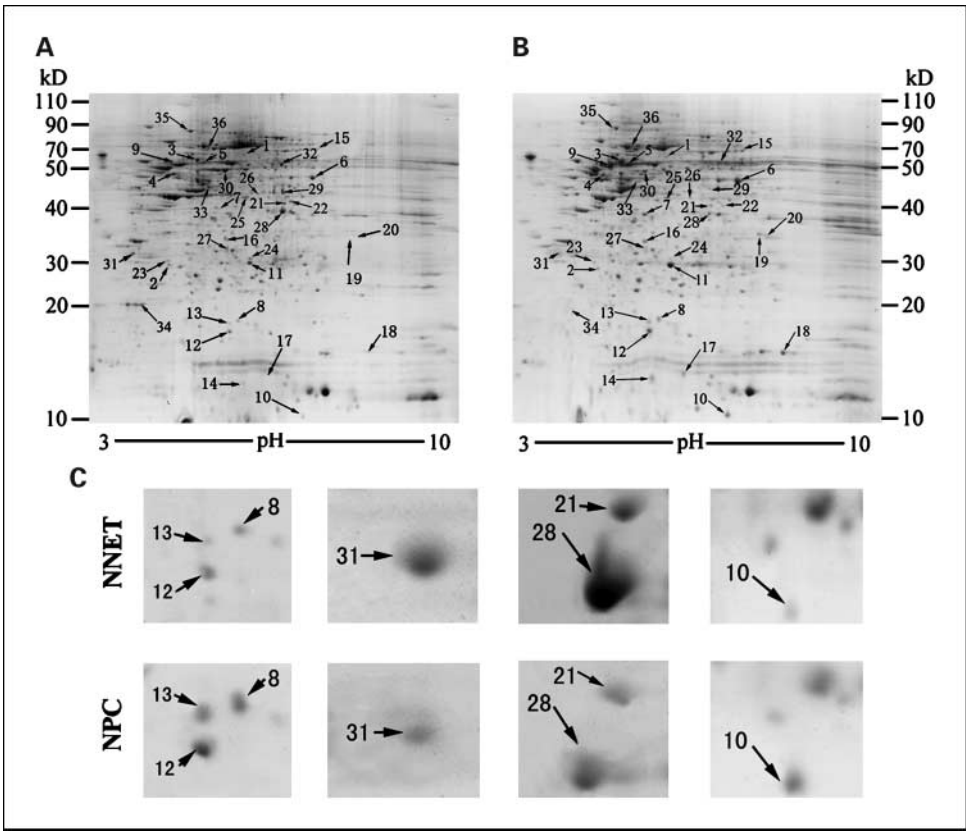

Fig. 2. Representative 2-DE maps of microdissected NNET (*A*) and NPC tissues (*B*). Arrows, protein spots of 36 differential protein spots identified by MS. *C,* close-up of the region of the gels showing partial differential expression proteins between the NNET and NPC tissues.

imported into the Mascot search engine with a MS/MS tolerance of ± 0.3 Da to search the Swiss-Prot database.

Western blotting. Twelve pairs of microdissected fresh NPC and NNET and four NPC cell lines (6-10B, 5-8F, CNE1, and CNE2) were used for Western blotting as previously described by us (23). 6-10B without metastatic potential and 5-8F with high metastatic potential were kindly provided by Dr. H.M. Wang of the Cancer Center, Sun Yat-sen University, China (25). Well differentiated CNE1 and poorly differentiated CNE2 are established NPC cell lines (26). Briefly, 40 μg of lysates were separated by 8% or 10% SDS-PAGE, and transferred to a polyvinylidene difluoride membrane. Blots were blocked with 5% nonfat dry milk for 2 h at room temperature, and then incubated with primary anti-stathmin, anti–14-3-3σ, or anti–annexin I antibody for 2 h at room temperature, followed by incubation with a horseradish peroxidase–conjugated secondary antibody for 1 h at room temperature. The signal was visualized with an enhanced chemiluminescence detection reagent and quantitated by densitometry using ImageQuant image analysis system (Storm Optical Scanner, Molecular Dynamics). The mouse anti–β-actin antibody (1:5,000, Sigma) was detected simultaneously as a loading control.

Immunohistochemistry. Immunohistochemistry was done on formalin-fixed and paraffin-embedded tissue sections using a standard immunohistochemical technique. Four-micrometer-thick tissue sections were deparaffinized in xylene, rehydrated in a graded ethanol series, and treated with an antigen retrieval solution (10 mmol/L sodium citrate buffer; pH 6.0). The sections were incubated with mouse monoclonal anti-stathmin antibody (dilution 1:100), goat polyclonal anti–14-3-3σ antibody (dilution 1:125), or rabbit polyclonal anti–annexin I antibody (dilution 1:400) overnight at 4°C, and were then incubated with a 1:1,000 dilution of biotinylated secondary antibody followed by avidin-biotin peroxidase complex (DAKO) according to the manufacturer's instructions. Finally, tissue sections were incubated with 3′,3′-diaminobenzidine (Sigma-Aldrich) until a brown color developed, and counterstained with Harris' modified hematoxylin. In negative controls, primary antibodies were omitted.

Evaluation of staining. Sections were blindly evaluated by two investigators in an effort to provide a consensus on staining patterns by light microscopy (Olympus). Stathmin, 14-3-3σ, and annexin I staining were assessed according to the methods described by Hara and Okayasu (27) with minor modifications. Each case was rated according to a score that added a scale of intensity of staining to the area of staining. At least 10 high-power fields were chosen randomly, and >1,000 cells were counted for each section. The intensity of staining was graded on the following scale: 0, no staining; 1+, mild staining; 2+, moderate staining; 3+, intense staining. The area of staining was evaluated as follows: 0, no staining of cells in any microscopic fields; 1+, <30% of tissue stained positive; 2+, between 30% and 60% stained positive; 3+, >60% stained positive. The minimum score when summed (extension + intensity) was therefore, 0, and the maximum, 6. A combined staining score (extension + intensity) of ≤2 was considered to be a negative staining (low staining); a score between 3 and 4 was considered to be a moderate staining; whereas a score between 5 and 6 was considered to be a strong staining.

Statistical analysis. Statistical analysis was done by using SPSS (version 13.0). The significant difference of stathmin, 14-3-3σ, and annexin I expression between the tumor and normal tissues, and primary and metastatic tumors was determined by using the *t* test. Significant differences between the expression of those three factors and clinical variables, including age, gender, histologic type/grade, primary tumor (T) stage, regional lymph node (N) metastasis, distant metastasis (M), clinical stage, and recurrence, were compared by the Mann-Whitney *U* test or ANOVA test. Survival rates (cumulative survival, cumulative survival curves) were obtained by the Kaplan-Meier method, and the differences (between the curves) were compared by log-rank tests. The deaths caused by NPC were considered as outcomes; the deaths by other causes were censored and the missing values were

replaced by the series mean method. A univariate analysis with Cox proportional hazards model was used to determine each identified prognostic factor; multivariate analysis with the Cox proportional hazards model was used to explore combined effects. A difference of $P < 0.05$ was considered statistically significant.

Results

2-DE maps of NPC and NNET. Proteins from three sets of pooled microdissected NPC and NNET were resolved by 2-DE, respectively, and stained with Coomassie blue. Two representative 2-DE maps from one set of pooled microdissected samples are shown in Fig. 2A and B. A total of 49 protein spots that have consistent differences (≥2-fold) between the tumor and normal tissues in triplicate experiments were chosen as differential protein spots and subjected to MS analysis, and 36 differential protein spots that have been identified by MS are marked with arrows in Fig. 2A and B. A close-up of the region of the gels showing partial differential expression proteins between the two types of tissues is shown in Fig. 2C.

Identification of differential proteins by MS. All 49 differential protein spots were excised from stained gels, *in situ* digested with trypsin, and analyzed by MALDI-TOF-MS and ESI-Q-TOF-MS. A total of 36 differential proteins were successfully identified (Table 1). Of the identified proteins, stathmin, nm23-H1, heat shock protein 27, vimentin, enolase, voltage-dependent anion channel 2, and guanine nucleotide binding protein, etc., were increased, whereas calcyphosine, annexin I, 14-3-3σ, squamous cell carcinoma antigen 1 (SCCA 1), keratin 8, and cathepsin D, etc., were decreased in NPC compared with NNET.

Validation of the identified proteins. To confirm the expression levels of the differential proteins identified by a proteomic approach, expression of the three identified proteins (stathmin, 14-3-3σ, and annexin I) in 12 pairs of microdissected NPC and NNET were detected by Western blotting. As shown in Fig. 3A and B, stathmin was significantly up-regulated, whereas 14-3-3σ and annexin I were significantly down-regulated in NPC versus NNET ($P < 0.01$), which confirms the results of proteomic analysis.

Table 1. Differential expression proteins between NPC and NNET identified by MALDI-TOF-MS and ESI-Q-TOF-MS

No.	Accession no.	Protein name	Fold change (NPC/NNET)
1	P17987	T-complex type molecular chaperone TCP1	↑2.00
2	P43487	Ran-binding protein 1	↑2.00
3	P10809	Chaperonin GroEL precursor	↑2.01
4	P06576	H+-transporting two-sector ATPase β chain precursor	↑2.01
5	P13647	Keratin 5	↑2.04
6	P31947	Enolase 1	↑2.09
7	Q53HK9	Acidic ribosomal protein P0	↑2.11
8	P15531	Metastasis inhibition factor/nm23 protein	↑2.25
9	P08670	Vimentin	↑2.29
10	P05109	Calgranulin A	↑2.51
11	P04792	HSP27 protein	↑2.57
12	Q96CE4	Stathmin	↑3.15
13	P37802	Transgelin-2	↑3.24
14	P06702	MRP-14 protein	↑3.24
15	Q6NTA2	HNRPL protein	↑3.56
16	P47756	Actin-capping protein β chain	↑5.09
17	O15540	Fatty acid binding protein	*
18	P62937	Peptidylprolyl isomerase A	*
19	Q5VWK3	VDAC2 protein	*
20	Q53HU2	Guanine nucleotide binding protein	*
21	P14550	Alcohol dehydrogenase	↓2.02
22	Q9NR45	*N*-acetylneuraminic acid phosphate synthase	↓2.03
23	P04632	Calpain small chain	↓2.03
24	P30084	Enoyl-CoA hydratase	↓2.11
25	P40121	Chain A, Ca_{2+}-binding mimicry in the crystal structure of Eu3+-bound mutant human macrophage capping protein Cap G	↓2.64
26	Q9UBS4	ER-associated Hsp40 cochaperone	↓3.08
27	P07339	Cathepsin D	↓3.17
28	Q5TZZ9	Annexin I	↓3.42
29	Q86W04	SCCA1	↓4.08
30	P05787	Keratin 8	↓4.42
31	Q53HR3	14-3-3σ	↓5.22
32	P00352	Aldehyde dehydrogenase	↓7.07
33	P05783	Keratin 18	↓7.50
34	Q13938	Calcyphosine	↓10.01
35	P55072	Transitional endoplasmic reticulum ATPase	†
36	P34931	Heat shock 70 kDa	†

*Expressed only in NPC.
† Expressed only in NNET.

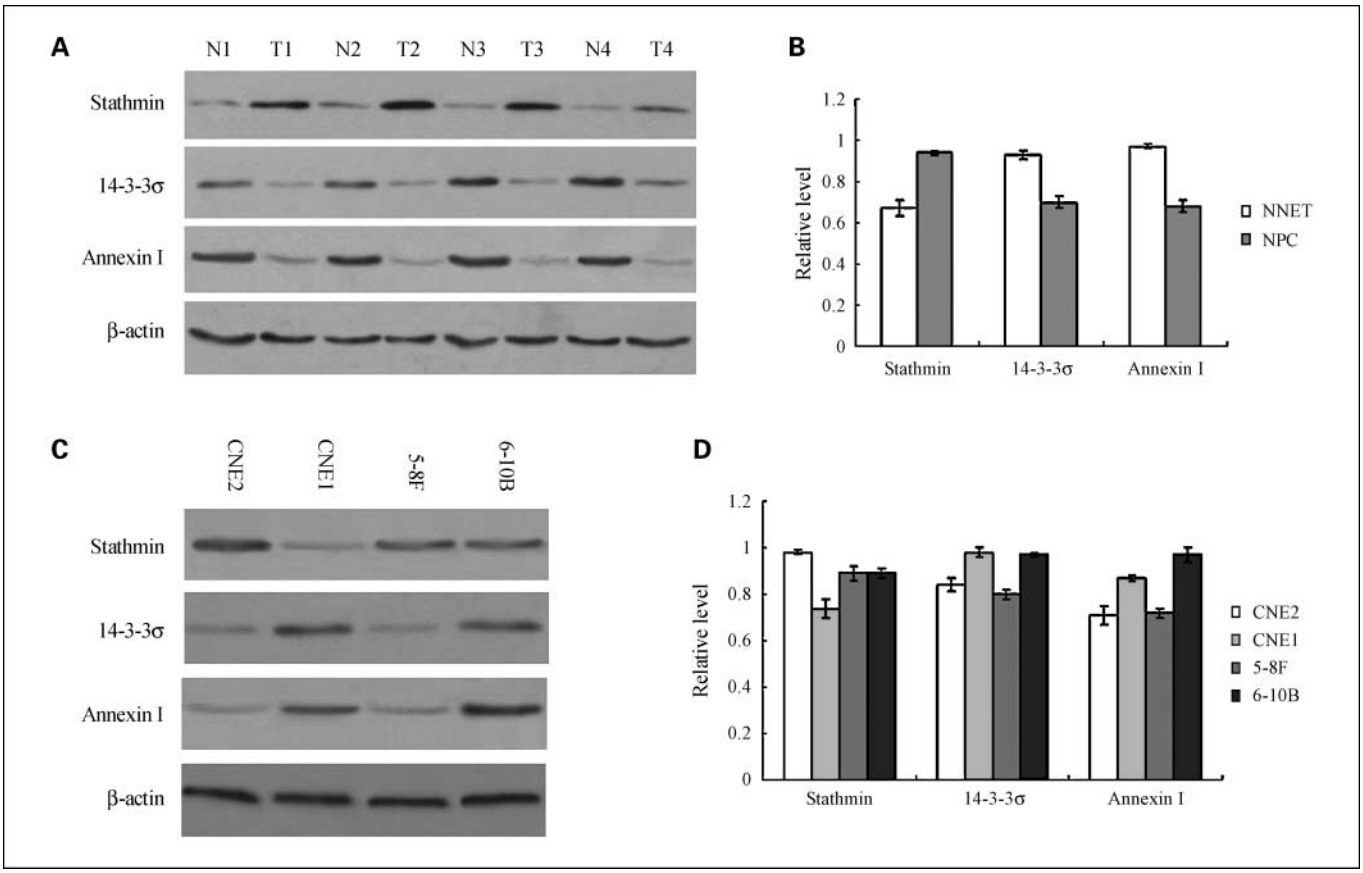

Fig. 3. Representative results of Western blotting of stathmin, 14-3-3σ, and annexin I in the tissue and cell samples. *A,* Western blotting shows changes in the expression levels of stathmin, 14-3-3σ, and annexin I in microdissected NPC tissue (*T*) and NNET (*N*). *B,* histogram of relative changes in the expression levels of the three proteins in the tumor and normal tissues as determined by densitometric analysis. *C,* Western blotting of the changes in the expression levels of stathmin, 14-3-3σ, and annexin I in NPC cell lines CNE2, CNE1, 5-8F, and 6-10B. *D,* histogram of relative changes in the expression levels of the three proteins in the four NPC cell lines as determined by densitometric analysis.

Expression of stathmin, 14-3-3σ, and annexin I in NPC cell lines. Western blotting was also done to detect the expression levels of stathmin, 14-3-3σ, and annexin I in the four NPC cell lines with different metastatic potentials or differentiated degrees. As shown in Fig. 3C and D, when compared with well-differentiated CNE1, the expression levels of 14-3-3σ and annexin I were significantly decreased in poorly differentiated CNE2, whereas the stathmin expression level was significantly increased ($P < 0.01$). There were also significantly higher expression levels of 14-3-3σ and annexin I in 6-10B without metastatic potential than those in 5-8F with high metastatic potential ($P < 0.01$), but no obvious change of stathmin expression level in 6-10B and 5-8F cell lines was observed. The results indicated that these three proteins were related to differentiation and/or metastatic potential of NPC cell lines.

Expression of stathmin, 14-3-3σ, and annexin I in NNET, and primary and metastatic NPC. Given the differential expressions of stathmin, 14-3-3σ, and annexin I in NPC and NNET, as well as NPC cell lines with different differentiated degrees or metastatic potentials, we further detected the expression of these three proteins using immunohistochemistry in 98 cases of primary NPC, 30 cases of NNET, and 20 cases of cervical LMNPC. As shown in Fig. 4 and Table 2, stathmin was significantly up-regulated, whereas 14-3-3σ and annexin I were significantly down-regulated in NPC versus NNET ($P < 0.01$). The expression levels of 14-3-3σ and annexin I in primary NPC were also significantly higher than those in LMNPC ($P < 0.01$), but no significant difference in the expression level of stathmin was observed in the primary NPC and LMNPC.

Correlation of stathmin, 14-3-3σ, and annexin I expression in primary NPC with clinicopathologic factors. Table 3 shows the correlation of several clinicopathologic factors with stathmin, 14-3-3σ, and annexin I expression status in 98 cases of primary NPC. Stathmin expression levels were correlated with histologic type/grade, primary tumor (T) stage, clinical stage, and recurrence ($P < 0.05$ or 0.01; Table 3). Type III (poorly differentiated) NPC showed a more intense immunoreactivity of stathmin compared with type I and II (well-moderately differentiated) NPC (Fig. 4; Table 3). Tumors with stathmin up-regulation tended to have a more advanced clinical stage and more frequent recurrences. The expression levels of 14-3-3σ and annexin I were correlated with histologic type/grade, clinical stage, recurrence, and regional lymph node and distant metastasis ($P < 0.05$ or 0.01; Table 3). Type I and II (well-moderately differentiated) NPC showed more intense immunoreactivity of 14-3-3σ and annexin I than type III (poorly differentiated) NPC (Fig. 4; Table 3). Tumors with the down-regulation of 14-3-3σ or annexin I tended to have a more advanced clinical stage, more frequent recurrence, and regional lymph node and distant metastasis. The expression levels of all

the three proteins did not correlate with the patients' age and gender, and stathmin expression level was not related to regional lymph node and distant metastasis (Table 3).

Survival analysis. Survival curves were calculated for a total of 98 cases of NPC patients. Two patients (2.0%) were lost during the follow-up. At the end of the study, 44 patients (44.9%) had died of NPC, 2 patients (2.0%) had died of unrelated causes, 50 patients (51.1%) were still alive, 29 patients (29.6%) had a recurrence of the disease, and 8 patients (8.2%) showed distant metastasis. The mean follow-up period was 48 $\pm$ 14.5 months. Using univariate analysis (Cox's proportional hazards model), the following variables were found to be significantly associated with prognosis: histologic type, clinical stage, recurrence, distant metastasis, and expression levels of stathmin, 14-3-3σ, and annexin I ($P < 0.05$; Table 4). Survival curves calculated by the Kaplan-Meier method and analyzed using the log-rank test showed that the survival rates of the patients with stathmin up-regulation or the down-regulation of 14-3-3σ and annexin I were significantly decreased ($P \leq 0.01$; Fig. 5). Multivariate analysis showed that recurrence, distant metastasis, and the expression levels of stathmin, 14-3-3σ, and annexin I had an independent prognostic effect on overall survival ($P < 0.01$; Table 5).

Discussion

NPC is one of the most common cancers in those of Chinese and Asian ancestry, and it poses one of the most serious public health problems in southern China and Southeast Asia (1). The 5-year survival rate for patients with NPC remains 50% to 60% despite advances in diagnosis and treatment, and the majority of patients succumb to invasion and metastasis (2, 12). Identification of new NPC biomarkers will be helpful for the diagnosis and treatment of NPC, and may provide new insights into its pathogenesis.

Because the functional molecules in cells are proteins, proteome analysis is believed to have an advantage over cDNA microarray for clinical use. Differential proteome analysis of tumor and normal tissues allows the identification of aberrantly expressed proteins in cancer that might provide key

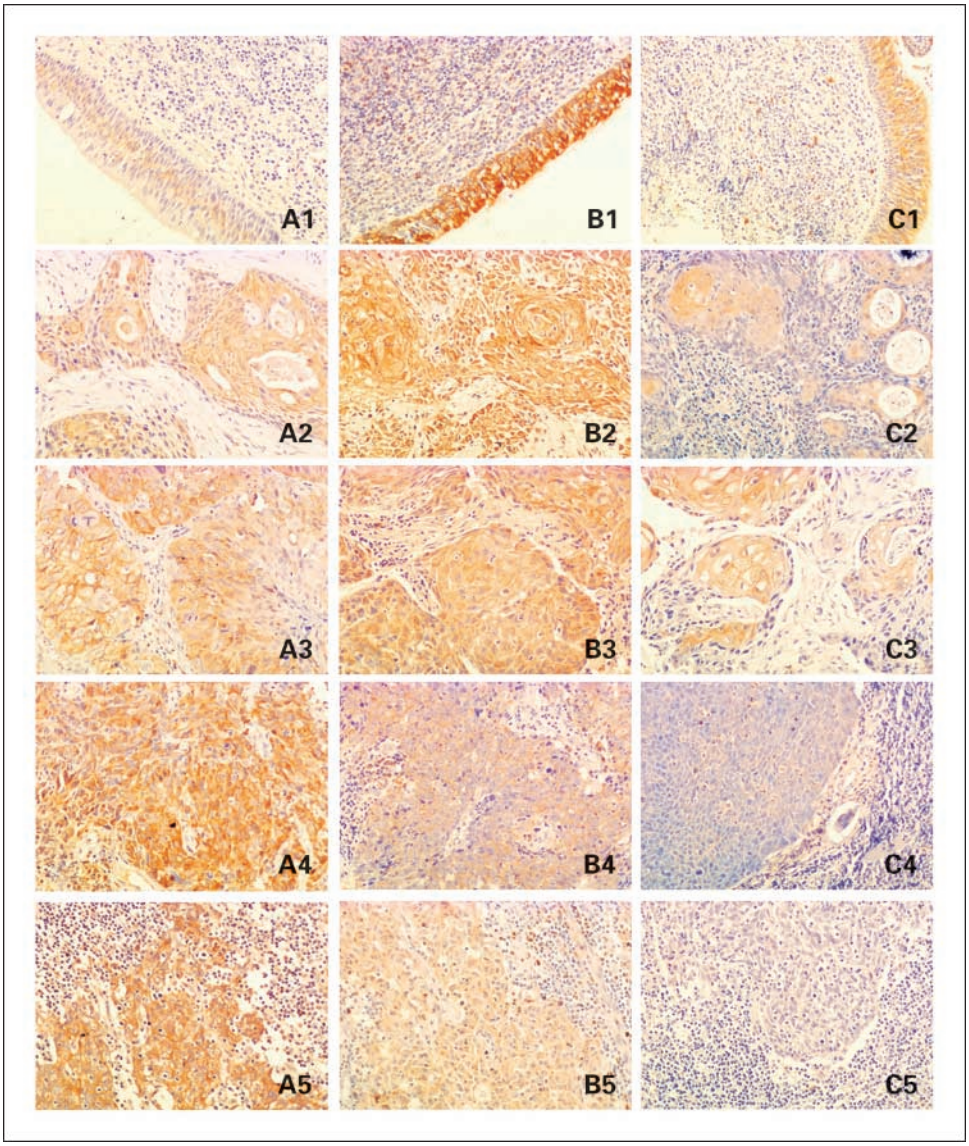

Fig. 4. Representative results of immunohistochemistry of stathmin, 14-3-3σ, and annexin I in the tissue specimens. *A,* immunohistochemistry of stathmin in NNET (*1*), WHO type I (*2*), type II (*3*), and type III (*4*) primary NPC, and LMNPC (*5*); *B,* immunohistochemistry of 14-3-3σ in NNET (*1*), WHO type I (*2*), type II (*3*), and type III (*4*) primary NPC, and LMNPC (*5*); *C,* immunohistochemistry of annexin 1 in NNET (*1*), WHO type I (*2*), type II (*3*), and type III (*4*) primary NPC, and LMNPC (*5*). Original magnification, $\times$200.

Table 2. The difference between stathmin, 14-3-3σ, and annexin I expression among NNET, primary NPC, and LMNPC

	n	Score			
		Low	Moderate	High	*P*
Stathmin					
NNET	30	28	2	0	0.000*
NPC	98	17	52	29	
LMNPC	20	4	6	10	0.303
14-3-3σ					
NNET	30	3	3	24	0.000*
NPC	98	27	32	39	
LMNPC	20	12	6	2	0.002†
Annexin I					
NNET	30	1	6	23	0.000*
NPC	98	33	42	23	
LMNPC	20	15	5	0	0.000†

*$P < 0.01$ by t test, NNET versus NPC.
†$P < 0.01$ by t test, NPC versus LMNPC.

information for finding biomarkers for the diagnosis and treatment of cancer as well as an understanding of carcinogenesis. However, differential proteomic study of NPC has been hampered by marked heterogeneity of NPC and NNET, and the acquired samples often do not contain the cells of interest. LCM has made it possible to isolate pure cell populations from heterogeneous tissue (18), which will increase the possibility and accuracy of screening for proteins associated with cancer by proteomic analysis using tissue samples (19–21).

In this study, LCM and proteomic approach were used to screen for differential proteins in NPC and NNET. A total of 36 differentially expressed proteins were identified by MS, and differential expression levels of three identified proteins (stathmin, 14-3-3σ, and annexin I) in NPC and NNET were confirmed by Western blotting, suggesting that the proteins identified by proteomic approach are actually differential expression proteins. Western blotting was also done to detect the expression levels of stathmin, 14-3-3σ, and annexin I in the four NPC cell lines with different metastatic potentials or differentiated degrees, the results of which indicated that the three proteins were related to the differentiation and/or metastatic potential of NPC cell lines. Because the differential expressions of stathmin, 14-3-3σ, and annexin I in NPC were confirmed and related to differentiation degree and/or metastatic potential of NPC cell lines, immunohistochemistry was done to detect the expression of stathmin, 14-3-3σ, and annexin I in NNET and primary and metastatic NPC tissue specimens, and the correlation of expression of the three proteins with clinicopathologic features and clinical outcomes were evaluated. The data showed that expression levels of

Table 3. Relationships between stathmin, 14-3-3σ, and annexin I expression and clinicopathologic factors

	n	Stathmin				14-3-3σ				Annexin I			
		0-2	3-4	5-6	*P*	0-2	3-4	5-6	*P*	0-2	3-4	5-6	*P*
Gender					0.530				0.799				0.745
Male	66	11	34	21		18	21	27		22	30	14	
Female	32	6	18	8		9	11	12		11	12	9	
Age (y)					0.240				0.428				0.772
≥50	30	7	16	7		8	13	9		10	12	8	
<50	68	10	36	22		19	19	30		23	30	15	
Histologic type (WHO)					0.005*				0.006*				0.000*
WHO I	5	3	2	0		0	1	4		0	2	3	
WHO II	13	4	8	1		1	3	9		1	4	8	
WHO III	80	10	42	28		26	28	26		32	36	12	
Primary tumor (T) stage					0.007*				0.366				0.784
T_1	12	5	6	1		3	5	4		5	4	3	
T_2	23	4	12	7		5	7	11		6	11	6	
T_3	49	6	32	11		13	15	21		18	21	10	
T_4	14	2	2	10		6	5	3		4	6	4	
Regional lymph node (N)metastasis					0.987				0.032*				0.018*
N_0	12	2	7	3		1	1	10		1	4	7	
N_1	17	3	8	6		6	4	7		9	5	3	
N_2	45	7	26	12		10	22	13		16	20	9	
N_3	24	5	11	8		10	5	9		7	13	4	
Distant metastasis (M)					0.255				0.002*				0.002*
M_0	90	16	49	25		21	30	39		26	41	23	
M_1	8	1	3	4		6	2	0		7	1	0	
Clinical stage					0.016*				0.001*				0.013*
II	10	5	3	2		1	2	7		2	2	6	
III	53	5	40	8		11	16	26		14	27	12	
IV	35	7	9	19		15	14	6		17	13	5	
Recurrence					0.000*				0.000*				0.000*
Negative	69	15	44	10		12	20	37		15	34	20	
Positive	29	2	8	19		15	12	2		18	8	3	

*$P < 0.05$ or 0.01 by Mann-Whitney U test or ANOVA test.

Table 4. Prognostic factors by univariate analysis (Cox's proportional hazards model)

Variables	Hazard ratio (95% confidence interval)	P
Age (≥50/<50)	0.096 (0.716-1.693)	0.660
Gender (male/female)	0.138 (0.754-1.749)	0.521
Tumor-node-metastasis staging (II/III/IV)	0.414 (1.098-2.086)	0.011*
WHO type (I/II/III)	0.400 (1.007-2.210)	0.046*
Recurrence (N/P)	2.583 (6.562-26.728)	0.000*
Metastasis (N/P)	1.527 (2.115-10.019)	0.000*
Stathmin (0-4/5-6)	2.383 (5.878-20.001)	0.000*
14-3-3σ (0-2/3-6)	-1.953 (0.086-0.235)	0.000*
Annexin I (0-2/3-6)	-3.013 (0.022-0.110)	0.000*

Abbreviations: N, negative; P, positive.
*P < 0.05 or 0.01.

stathmin, 14-3-3σ, and annexin I were significantly correlated with several clinicopathologic variables and prognosis of NPC.

Stathmin/oncoprotein 18 (Op18), a 19 kDa cytosolic protein that promotes microtubule depolymerization in a cell cycle– and phosphorylation-dependent manner, is a key regulator of cell division and differentiation through its influence on microtubule dynamics (28), and simultaneously, it is a relay integrating diverse intracellular signaling pathways (29). Stathmin has attracted the attention of many investigators because of its overexpression in various types of human malignancies such as breast carcinoma (30), lung adenocarcinoma (31), and oral squamous cell carcinoma (32). Overexpressed Op18 has been associated with the poor differentiation and prognosis of several cancers, and was thought to be a biomarker for tumor differentiation and prognosis (30–32). Because stathmin, a ubiquitous microtubule-regulatory protein, is overexpressed in many types of cancers, and drugs that inhibit cell division by interfering with microtubule function are widely used in cancer chemotherapy, stathmin provides an attractive molecular target for disrupting the mitotic apparatus and arresting the growth of cancer cells. Indeed, several studies have shown that inhibition of stathmin expression in cancer cells could interfere with their orderly progression through the cell cycle, abrogate their transformed phenotype (33), and increase their chemosensitivity (34). However, the expression status and significance of stathmin in NPC have not been previously established. In the present study, our results showed for the first time that stathmin was up-regulated in NPC versus NNET, and its up-regulation was associated with the differentiation and prognosis of this disease as well. The data suggested that stathmin might be a biomarker for differentiation and prognosis of NPC, and a potential therapeutic target for this cancer.

14-3-3 proteins are a family of abundant, highly conserved, and widely expressed 28 to 33 kDa acidic polypeptides (35). Seven isoforms including β, γ, ε, σ, ζ, θ, and η have been identified in mammals. 14-3-3σ was originally characterized as a human mammary epithelium-specific marker 1 (HME1), primarily expressed in epithelial cells, and gradually up-regulated during epithelial cell differentiation (36). Among the seven isoforms, 14-3-3σ, that is up-regulated by p53 in response to DNA damage, is a negative regulator of cell cycle checkpoints and is thought to be a potential tumor-suppressor protein (35). 14-3-3σ up-regulation could antagonize oncogene-mediated cell growth and transformation in breast cancer cell lines (37), whereas its down-regulation allowed primary human keratinocytes to grow and immortalize (38). Accumulative studies showed that 14-3-3σ expression was decreased in various types of human epithelial cancer due to CpG island hypermethylation, which was associated with the development and progression of cancer (39–41). It was also reported that 14-3-3σ down-regulation is an independent prognosis factor for patients with gastrointestinal and breast cancers (42, 43). A recent study has shown that overexpression of 14-3-3σ in NPC cell lines could reduce the tumor volume in nude mice, which provided an insight into the role of 14-3-3σ in NPC and suggested that modulating 14-3-3σ activity might be useful in the treatment of this disease (44). In the present study, our results, for the first time, showed that 14-3-3σ was down-regulated in primary NPC versus NNET, and metastatic NPC versus primary NPC, and its down-regulation was associated with differentiation, metastasis, and prognosis of this disease. The data suggested that 14-3-3σ might be a biomarker for differentiation, metastasis, and prognosis of NPC, and a potential therapeutic target for this cancer.

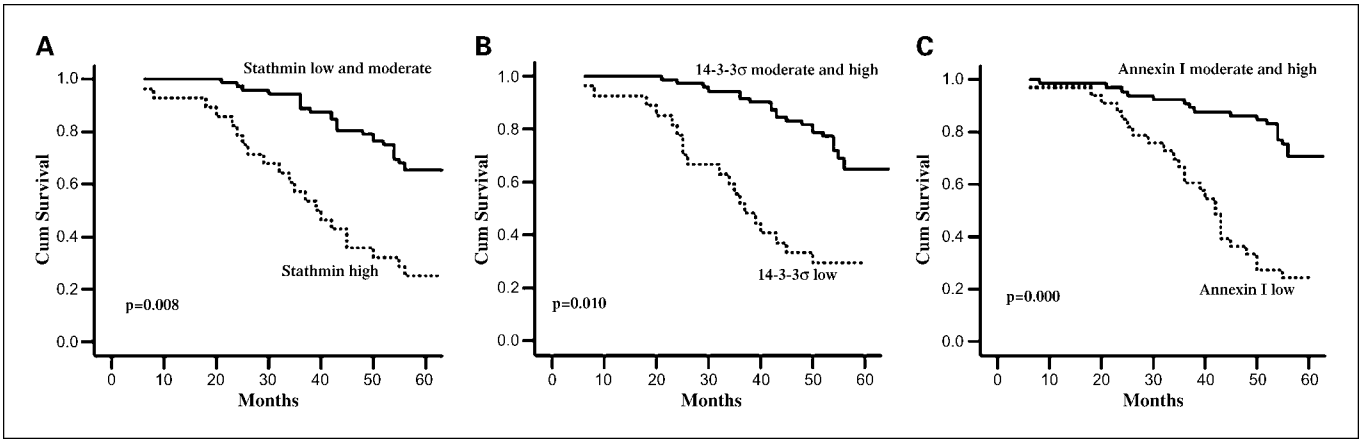

Fig. 5. Kaplan-Meier survival curves according to expression levels of stathmin (P = 0.008; *A*), 14-3-3σ (P = 0.010; *B*), and annexin I (P = 0.000; *C*) in primary NPC.

Table 5. Significant prognostic factors by multivariate analysis (Cox's proportional hazards model)

Variables	Hazard ratio (95% confidence interval)	P
Tumor-node-metastasis staging (II/III/IV)	0.134 (0.607-1.259)	0.471
WHO type (I/II/III)	0.410 (0.419-1.052)	0.081
Recurrence (N/P)	1.717 (2.497-12.412)	0.000*
Metastasis (N/P)	1.256 (1.496-8.235)	0.004*
Stathmin (0-2/3-4/5-6)	0.706 (1.257-3.263)	0.004*
14-3-3σ (0-2/3-4/5-6)	-0.490 (0.428-0.875)	0.007*
Annexin I (0-2/3-4/5-6)	-0.820 (0.270-0.717)	0.001*

Abbreviations: N, negative; P, positive.
*$P < 0.05$ or 0.01.

Annexins are a structurally related family of 37 to 39 kDa calcium- and phospholipid-binding proteins that have been implicated in a broad range of molecular and cellular processes including the modulation of phospholipase A2 and kinase activities in signal transduction, the maintenance of cytoskeleton and extracellular matrix integrity, tissue growth and differentiation, inflammation, and blood coagulation, etc. (45). Annexins are commonly dysregulated in cancer, and their frequent down-regulation has suggested a possible homeostatic or tumor suppressor role (46). Annexin I, a member of the annexin superfamily, is well expressed in a wide range of tissues and is specifically implicated in epithelial differentiation and growth regulation. It is markedly down-regulated in certain cancers such as esophageal, prostate, and breast carcinomas (47, 48). It was reported that down-regulation of annexin I was associated with poor differentiation of head and neck cancer (49, 50). In this study, the results showed that annexin I was down-regulated in primary NPC versus NNET, and metastatic NPC versus primary NPC, and its down-regulation was associated with differentiation, metastasis, and prognosis of this disease. Thus, annexin I might be a biomarker for differentiation, metastasis, and prognosis of NPC.

In summary, we identified 36 differential expression proteins between NPC and NNET using a proteomic approach coupled with LCM. We further showed that three differential proteins (stathmin, 14-3-3σ, and annexin I) are potential biomarkers for differentiation and prognosis of NPC, and might contribute to NPC carcinogenesis. The findings reported here could have clinical value in distinguishing histologic grades, predicting the prognosis of NPC, and identifying NPC patients that are at high risk of progression and recurrence.

References

1. Yu MC, Yuan JM. Epidemiology of nasopharyngeal carcinoma. Semin Cancer Biol 2002;12:421–9.
2. Vokes EE, Liebowitz DN, Weichselbaum RR. Nasopharyngeal carcinoma. Lancet 1997;350:1087–91.
3. Raab-Traub N. Epstein-Barr virus in the pathogenesis of NPC. Semin Cancer Biol 2002;12:431–41.
4. Yau WL, Lung HL, Zabarovsky ER, et al. Functional studies of the chromosome 3p21.3 candidate tumor suppressor gene BLU/ZMYND10 in nasopharyngeal carcinoma. Int J Cancer 2006;119:2821–6.
5. Hui AB, Or YY, Takano H, et al. Array-based comparative genomic hybridization analysis identified cyclin D1 as a target oncogene at 11q13.3 in nasopharyngeal carcinoma. Cancer Res 2005;65:8125–33.
6. Kwong J, Lo KW, To KF, et al. Promoter hypermethylation of multiple genes in nasopharyngeal carcinoma. Clin Cancer Res 2002;8:131–7.
7. Hu LF, Eiriksdottir G, Lebedeva T, et al. Loss of heterozygosity on chromosome arm 3p in nasopharyngeal carcinoma. Genes Chromosomes Cancer 1996;17:118–26.
8. Deng L, Jing N, Tan G, et al. A common region of allelic loss on chromosome region 3p25.3-26.3 in nasopharyngeal carcinoma. Genes Chromosomes Cancer 1998;23:21–5.
9. Huang DP, Lo KW, van Hasselt CA, et al. A region of homozygous deletion on chromosome 9p21-22 in primary nasopharyngeal carcinoma. Cancer Res 1994;54:4003–6.
10. Xiong W, Zeng ZY, Xia JH, et al. A susceptibility locus at chromosome 3p21 linked to familial nasopharyngeal carcinoma. Cancer Res 2004;64:1972–4.
11. Feng BJ, Huang W, Shugart YY, et al. Genome-wide scan for familial nasopharyngeal carcinoma reveals evidence of linkage to chromosome 4. Nat Genet 2002;31:395–9.
12. Ahmad A, Stefani S. Distant metastases of nasopharyngeal carcinoma: a study of 245 male patients. J Surg Oncol 1986;33:194–7.
13. Wong MM, Lye MS, Cheng HM, et al. Epstein-Barr virus serology in the diagnosis of nasopharyngeal carcinoma. Asian Pac J Allergy Immunol 2005;23:65–7.
14. Cho WC, Yip TT, Yip C, et al. Identification of serum amyloid A protein as a potentially useful biomarker to monitor relapse of nasopharyngeal carcinoma by serum proteomic profiling. Clin Cancer Res 2004;10:43–52.
15. Song LB, Zeng MS, Liao WT, et al. Bmi-1 is a novel molecular marker of nasopharyngeal carcinoma progression and immortalizes primary human nasopharyngeal epithelial cells. Cancer Res 2006;66:6225–32.
16. Qian CN, Guo X, Cao B, et al. Met protein expression level correlates with survival in patients with late-stage nasopharyngeal carcinoma. Cancer Res 2002;62:589–96.
17. Sriuranpong V, Mutirangura A, Gillespie JW, et al. Global gene expression profile of nasopharyngeal carcinoma by laser capture microdissection and complementary DNA microarrays. Clin Cancer Res 2004;10:4944–58.
18. Emmert-Buck MR, Bonner RF, Smith PD, et al. Laser capture microdissection. Science 1996;274:998–1001.
19. Neubauer H, Clare SE, Kurek R, et al. Breast cancer proteomics by laser capture microdissection, sample pooling, 54-cm IPG IEF, and differential iodine radioisotope detection. Electrophoresis 2006;27:1840–52.
20. Li C, Hong Y, Tan YX, et al. Accurate qualitative and quantitative proteomic analysis of clinical hepatocellular carcinoma using laser capture microdissection coupled with isotope-coded affinity tag and two-dimensional liquid chromatography mass spectrometry. Mol Cell Proteomics 2004;3:399–409.
21. Shekouh AR, Thompson CC, Prime W, et al. Application of laser capture microdissection combined with two-dimensional electrophoresis for the discovery of differentially regulated proteins in pancreatic ductal adenocarcinoma. Proteomics 2003;3:1988–2001.
22. Shanmugaratnam K, Sobin LH. Histological typing of tumors of the upper respiratory tract and ear. In: World Health Organization International Histological Classification of Tumors. 2nd ed. Berlin: Springer; 1991. p. 32–33.
23. Yang Y, Xiao Z, Chen Z, et al. Proteome analysis of multidrug resistance in vincristine-resistant human gastric cancer cell line SGC7901/VCR. Proteomics 2006;6:2009–21.
24. Candiano G, Bruschi M, Musante L, et al. P.G. Blue silver: a very sensitive colloidal Coomassie G-250 staining for proteome analysis. Electrophoresis 2004;25:1327–33.
25. Song LB, Yan J, Jian SW, et al. Molecular mechanisms of tumorigenesis and metastasis in nasopharyngeal carcinoma cell sublines. Ai Zheng 2002;21:158–62.
26. Cheung H, Jin D, Ling MT, et al. Mitotic arrest deficient 2 expression induces chemosensitization to a DNA-damaging agent, Cisplatin, in nasopharyngeal carcinoma cells. Cancer Res 2005;65:1450–8.
27. Hara A, Okayasu I. Cyclooxygenase-2 and inducible nitric oxide synthase expression in human astrocytic gliomas: correlation with angiogenesis and prognostic significance. Acta Neuropathol 2004;108:43–8.
28. Rubin CI, Atweh GF. The role of oncoprotein 18 in the regulation of the cell cycle. J Cell Biochem 2004;93:242–50.
29. Larsson N, Marklund U, Gradin HM, et al. Control of microtubule dynamics by oncoprotein 18: dissection of the regulatory role of multisite phosphorylation during mitosis. Mol Cell Biol 1997;17:5530–9.
30. Brattsand G. Correlation of oncoprotein 18/stathmin expression in human breast cancer with established prognostic factors. Br J Cancer 2000;83:311–8.
31. Chen G, Wang H, Gharib TG, et al. Overexpression of oncoprotein 18 correlates with poor differentiation in lung adenocarcinomas. Mol Cell Proteomics 2003;2:107–16.
32. Kouze Y, Uzawa K, Koike H, et al. Overexpression of stathmin in oral squamous-cell carcinoma: correlation with tumour progression and poor prognosis. Br J Cancer 2006;94:717–23.

33. Mistry SJ, Atweh GF. Role of stathmin in the regulation of the mitotic spindle: potential applications in cancer therapy. Mt Sinai J Med 2002;69:299–304.
34. Iancu C, Mistry SJ, Arkin S, et al. Taxol and antistathmin therapy: a synergistic combination that targets the mitotic spindle. Cancer Res 2000;60:3537–41.
35. Mhawech P. 14-3-3 proteins—an update. Cell Res 2005;15:228–36.
36. Prasad GL, Valverius EM, McDuffie E, et al. Complementary DNA cloning of a novel epithelial cell marker protein, HME1, that may be down-regulated in neoplastic mammary cells. Cell Growth Differ 1992;3:507–13.
37. Laronga C, Yang HY, Neal C, et al. Association of the cyclin-dependent kinases and 14-3-3σ negatively regulates cell cycle progression. J Biol Chem 2000;275:23106–12.
38. Dellambra E, Golisano O, Bondanza S, et al. Down-regulation of 14-3-3σ prevents clonal evolution and leads to immortalization of primary human keratinocytes. J Cell Biol 2000;149:1117–30.
39. Akahira J, Sugihashi Y, Suzuki T, et al. Decreased expression of 14-3-3σ is associated with advanced disease in human epithelial ovarian cancer: its correlation with aberrant DNA methylation. Clin Cancer Res 2004;10:2687–93.
40. Uchida D, Begum NM, Almofti A, et al. Frequent downregulation of 14-3-3σ protein and hypermethylation of 14-3-3σ gene in salivary gland adenoid cystic carcinoma. Br J Cancer 2004;91:1131–8.
41. Iwata N, Yamamoto H, Sasaki S, et al. Frequent hypermethylation of CpG islands and loss of expression of the 14-3-3σ gene in human hepatocellular carcinoma. Oncogene 2000;19:5298–302.
42. Perathoner A, Pirkebner D, Brandacher G, et al. 14-3-3σ expression is an independent prognostic parameter for poor survival in colorectal carcinoma patients. Clin Cancer Res 2005;11:3274–9.
43. Tanaka K, Hatada T, Kobayashi M, et al. The clinical implication of 14-3-3σ expression in primary gastrointestinal malignancy. Int J Oncol 2004;25:1591–7.
44. Yang H, Zhao R, Lee MH. 14-3-3σ, a p53 regulator, suppresses tumor growth of nasopharyngeal carcinoma. Mol Cancer Ther 2006;5:253–9.
45. Gerke V, Moss SE. Annexins: from structure to function. Physiol Rev 2002;82:331–71.
46. Xin W, Rhodes DR, Ingold C, et al. Dysregulation of the annexin family protein family is associated with prostate cancer progression. Am J Pathol 2003;162:255–61.
47. Paweletz CP, Ornstein DK, Roth MJ, et al. Loss of annexin 1 correlates with early onset of tumorigenesis in esophageal and prostate carcinoma. Cancer Res 2000;60:6293–7.
48. Shen D, Nooraie F, Elshimali Y, et al. Decreased expression of annexin A1 is correlated with breast cancer development and progression as determined by a tissue microarray analysis. Hum Pathol 2006;37:1583–91.
49. Garcia Pedrero JM, Fernandez MP, Morgan RO, et al. Annexin A1 down-regulation in head and neck cancer is associated with epithelial differentiation status. Am J Pathol 2004;164:73–9.
50. Rodrigo JP, Garcia-Pedrero JM, Fernandez MP, et al. Annexin A1 expression in nasopharyngeal carcinoma correlates with squamous differentiation. Am J Rhinol 2005;19:483–7.

Clinical Cancer Research

Identification of Novel Nasopharyngeal Carcinoma Biomarkers by Laser Capture Microdissection and Proteomic Analysis

Ai-Lan Cheng, Wei-Guo Huang, Zhu-Chu Chen, et al.

Clin Cancer Res 2008;14:435-445.